

Critical dynamics on a large human Open Connectome network

Géza Ódor

*MTA-EK-MFA, Research Center for Energy, Hungarian Academy of Sciences and
P. O. Box 49, H-1525 Budapest, Hungary*

(Dated: March 18, 2019)

Extended numerical simulations of threshold models have been performed on a human brain network with $N = 836733$ connected nodes available from the Open Connectome project. While in case of simple threshold models a sharp discontinuous phase transition without any critical dynamics arises, variable thresholds models exhibit extended power-law scaling regions. This is attributed to fact that Griffiths effects, stemming from the topological/interaction heterogeneity of the network, can become relevant if the input sensitivity of nodes is equalized. I have studied the effects of link directness, as well as the consequence of inhibitory connections. Non-universal power-law avalanche size and time distributions have been found with exponents agreeing with the values obtained in electrode experiments of the human brain. The dynamical critical region occurs in an extended control parameter space without the assumption of self organized criticality.

PACS numbers: 05.70.Ln 89.75.Hc 87.19.lj

I. INTRODUCTION

Theoretical and experimental research provides many signals for the brain to operate in a critical state between sustained activity and an inactive phase [1–4]. Critical systems exhibit optimal computational properties, suggesting why the nervous system would benefit from such mode [5]. For being critical certain control parameters need to be tuned, leading to the obvious question why and how this is achieved. This question is well known in statistical physics, the theory of self-organized criticality (SOC) of homogeneous systems has a long history since the pioneering work of [6]. In case of competing fast and slow processes SOC systems can self-tune themselves in the neighborhood of a phase transition point [7]. Many simple models homogeneous have been suggested to describe power-laws (PL) and various other critical phenomena, sometimes even without identifying such processes that could be responsible for SOC. Alternatively, it has recently been proposed that living systems might also self-tune to criticality as the consequence of evolution and adaptation [8].

Real systems, however, are highly inhomogeneous and one must consider if heterogeneity are weak enough to use homogeneous models to describe them. Heterogeneity are also called disorder in statistical physics and they can lead to such rare-region (RR) effects that smear the phase transitions [9]. RR-s can have various effects depending on their relevancy They can make a discontinuous transition continuous [10, 11] or generate so-called Griffiths phases (GP) [12] or completely smear a singular phase transition. In case of GP-s critical-like power-law dynamics appears over an extended region around the critical point, causing slowly decaying auto-correlations and burstiness [13]. Such behavior was proposed to be the reason for the working memory in the brain [14]. Furthermore, in GP-s the susceptibility is infinite for an entire range of control parameters near the critical point, providing a high sensitivity to stimuli beneficial for information processing.

Therefore, studying the effects of heterogeneity is a very important issue in models of real system, in particular in neuroscience. It has been conjectured that network heterogeneity can cause GP-s if the topological (graph) dimension D , defined by

$$N_r \sim r^D, \quad (1)$$

where N_r is the number of (j) nodes within topological distance $r = d(i, j)$ from an arbitrary origin (i), is finite ([15]). This hypothesis is pronounced for the Contact Process [16], but subsequent studies found numerical evidence for its validity in case of more general spreading models [17–19]. Recently GP-s were reported in synthetic brain networks [20–22] with finite D . At first sight this seems to exclude relevant disorder effects in the so called small-world network models. However, in finite systems Griffiths effects are observable in finite time windows even if $D \rightarrow \infty$ in the $N \rightarrow \infty$ limit [23]. In such complex networks the phase transition region with high susceptibility and PL-s is extended, without the need of a self-tuning SOC mechanism.

Very recently we have studied the topological behavior of large human connectome networks and found that contrary to the small world network coefficients they exhibit topological dimension slightly above $D = 3$ [24]. This is due to the $D = 3$ dimensional embedding space and the weak long-range connections and warrants to see heterogeneity effects in dynamical models defined on them. These graphs also contain node connection data, thus one can study the combined effect of topological and interaction disorder, assuming a quasi static network.

This work provides a numerical analysis based on huge data sets of the Open Connectome project (OCP) [25] obtained by Diffusion Tensor Imaging (DTI) [26] describing *structural brain connectivity*. Earlier studies of the structural network were much smaller sized, for example the one obtained by Sporns and collaborators, using diffusion imaging techniques [27, 28], consists of a highly coarse-grained mapping of anatomical connections in the human brain, comprising $N = 998$ brain areas and the fiber tract densities between them. The graph used here comprises $N = 848848$ nodes allowing one to run extensive dynamical simulations on present days CPU/GPU clusters.

II. MODELS AND METHODS

Currently, connectomes can be estimated in humans at 1 mm^3 scale using a combination of diffusion weighted magnetic resonance imaging, functional magnetic resonance imaging and structural magnetic resonance imaging scans. The large graph "KKI-18" used here is generated by the MIGRAINE method as described in [29]. Note that OCP graphs describe symmetric, weighted, but not single connected networks due to the image processing technique. The investigated graph exhibits a single giant component of size $N = 836733$ nodes (out of $N = 848848$) and several small sub-components, ignored here, to disregard an unrealistic brain network scenario. In case of full symmetrization it has $E = 8304786$ edges, but to make it more realistic I removed connections randomly, such that 20% of them became directed. This value is in between the 5/126 of [30] and 33% reported in [31]. I shall also discuss the relevancy of this edge asymmetry.

The weights of this graph vary between 1 and 854 and their distribution is shown on Fig. 1. Following a sharp drop one can observe a PL region for $20 < w < 200$ with cutoff at large weights. The average weight of this distribution is $\simeq 5$. Note, that the average degree of this graph is $\langle 156 \rangle$ [24], while the average of the sum of the incoming weights of nodes is $\langle W_i \rangle = 1/N \sum_i \sum_j w_{ij} = 448$.

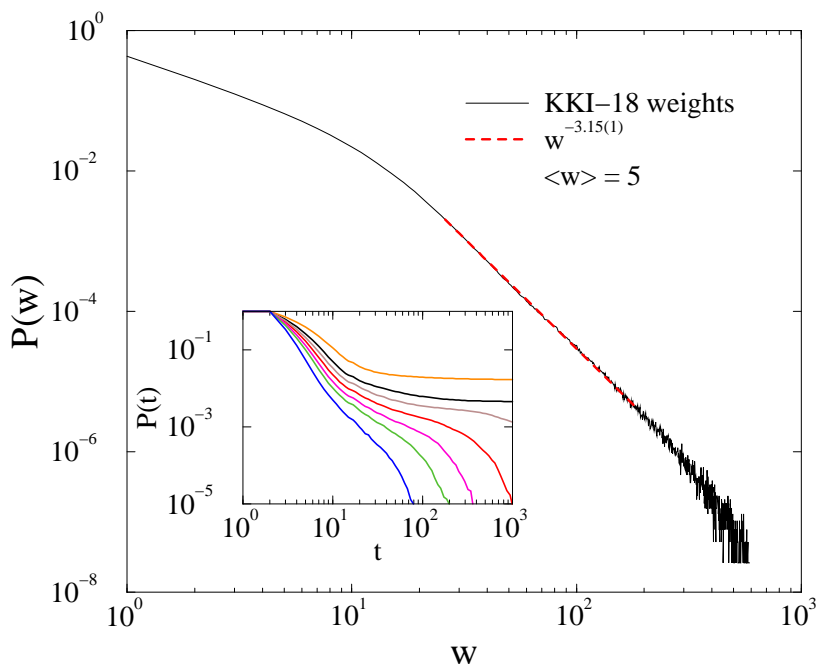


FIG. 1: Link weight distribution of the KKI-18 OCP graph. Dashed line: a PL fit for intermediate w -s. Inset: Survival probability in the $k = 6$ threshold model near the transition point for $\lambda = 0.003$, $\nu = 0.3, 0.4, 0.45, 0.5, 0.55, 0.6, 0.7$ (top to bottom curves).

I used a two-state ($x_i = 0$ or 1) dynamical spreading-type of model to describe the propagation, branching and annihilation of activity on the network. This threshold model is similar to that of ref. [32]. The dynamical process is started by activating a randomly selected site. At each network update all nodes are visited and tested if the sum of weights of neighbors (w_j) of node i reaches a given threshold value

$$\sum_j w_j > K. \quad (2)$$

If this condition is satisfied a node activation is attempted with probability λ . Alternatively, an active node is deactivated with probability ν . The new states of nodes are overwritten only after a full network update, i.e. a synchronous update is performed at discrete time steps. The updating process continues as long as there are active sites or up to a maximum time limit $t \leq 10^5$ Monte Carlo sweeps (MCs). In case the system is fallen to inactivity the actual time step is stored in order to calculate the survival probability $P(t)$ of runs. The average activity: $\rho(t) = 1/N \sum_{i=1}^N x_i$ and the number of activated nodes during the avalanche $s = \sum_{i=1}^N \sum_{t=1}^T x_i$ of duration T is calculated at the end of the simulations. This stochastic cellular automaton type of updating is not expected to affect the dynamical scaling behavior [22] and provides a possibility for network-wise parallel algorithms. Measurements on 10^6 to 10^7 independent runs, started from randomly selected, active initial sites were averaged over at each control parameter value.

By varying the control parameters, K , λ and ν I attempted to find a critical point between an active and an absorbing steady state. At a critical transition point the survival probability is expected to scale asymptotically as

$$P(t) \propto t^{-\delta}, \quad (3)$$

where δ is the survival probability exponent [35] and which can be related to the avalanche (total number of active sites during the spreading experiment) duration scaling

$$p(t) \propto t^{-\tau_t}, \quad (4)$$

with the scaling relation $\tau_t = 1 + \delta$ [36]. In seed experiments initial number of active sites scales as

$$N(t) \propto t^\eta, \quad (5)$$

with the exponent η , related to the avalanche size distribution

$$p(s) \propto t^{-\tau}, \quad (6)$$

via the scaling law

$$\tau = (1 + \eta + 2\delta)/(1 + \eta + \delta) \quad (7)$$

[36]. To see the corrections to scaling I also determined the local slopes of the dynamical exponents δ and η as the discretized, logarithmic derivative of (3) and (5). The effective exponent of δ is measured as

$$\delta_{\text{eff}}(t) = -\frac{\ln P(t) - \ln P(t')}{\ln(t) - \ln(t')}, \quad (8)$$

using $t - t' = 8$ and similarly can one define $\eta_{\text{eff}}(t)$.

As the OCP graph is very inhomogeneous it appears that for a given set of control parameters only the hub neurons can be activated and the weakly coupled neurons do not play any role. This is rather unrealistic and is against the local sustained activity requirement for of the brain [32]. Indeed there is some evidence that neurons have certain adaptation to their input excitation levels [33] and can be modeled by node dependent thresholds [34]. To model neurons with variable thresholds such that nodes exhibit the same sensitivity I used modified weights by normalizing them as $w'_i = w_i / \sum_{j \in \text{neighb. of } i} w_j$. Although the update rules are unchanged I shall call such simulations "variable threshold model" studies.

III. DYNAMICAL SIMULATION RESULTS

It is well known that in branching and annihilating models with multi-particle (A) reactions $mA \rightarrow (m+k)A$, $nA \rightarrow (n-l)A$ for $m > n$ the phase transition in the high dimensional, mean-field limit is first order [37]. Therefore, it can be expected that for threshold models with $K > 1$, near and above the the upper critical dimension, which is expected to be $d_c \leq 4$ we observe discontinuous transitions. First I run the threshold model on a homogeneous 3-dimensional lattice with $N = 10^6$ nodes and periodic boundary conditions. I tested the low: $K = 1, 2, 3, 6$ threshold cases, being the most possible candidates for PL dynamics. However, for high branching probability, where an efficient neural network should work, a fast evolution to the active state occurs for any ν . Thus transitions and PL-s cannot be found for any high λ values. On the other hand for $K \gg 1$ transitions can occur at high λ , but they are very sharp, in agreement with the results of [37], thus we cannot see the PL dynamics either. The avalanche size distributions decay as $p(s) \propto 1/s$. According to the relation (7) this corresponds to $\delta = 0$, when the $P(t)$ does not change asymptotically.

Next, I performed simulations of the threshold model on the KKI-18 graph with $K = 1, 2, 6$, since for larger K -s we don't expect criticality. I did not find PL behavior in the survival time distributions. Instead, one can observe an exponentially fast drop of $P(t)$ to zero or to some finite value, depending on the control parameters. Discontinuous transition occurs at very low λ -s, as shown in the inset of Fig. 1. Therefore, heterogeneity of the OCP graph are not strong enough to round the discontinuous transition, observed on the homogeneous lattice. It appears that large hubs, with many incoming weights, determine the behavior of the whole system, while other nodes do not play a role as we drive it from active to inactive state. These hubs keep the system active or inactive, ruling out the occurrence of local rare-region effects like in case of SIS on SF networks [23].

Therefore, I turn now towards the simulations of variable threshold models. To restrict the control parameter space I fixed $\lambda \simeq 1$, to mimic an efficient brain model. Transitions could be found for $K < 0.5$, for higher thresholds the models evolve to inactive phase for any ν -s. For the time being I set $K = 0.25$. Fig. 2 suggests a phase transition at $\nu = 0.95$ and $\lambda = 0.88(2)$, above which $P(t)$ curves evolve to finite constant values. It is very hard to locate clearly, since the evolution slows down and periodic oscillations add (inset of Fig. 2). The straight lines on the log. plot of δ_{eff} at $\lambda \simeq 1$ suggest ultra slow dynamics as in case of a strong disorder fixed point [9]. Indeed a logarithmic fitting at criticality results in $P(t) \simeq \ln(t)^{-3.5(3)}$, which is rather close to the the 3-dimensional strong disorder universal behavior [38, 39]. Simulations started from fully active sites show analogous decay curves for the density of active sites $\rho(t)$ expressing a rapidity reversal symmetry, characteristic of the Directed Percolation universality class [40], governing the critical behavior of such models without disorder [41]. However, for the graph dimension of this network $D \simeq 3.2$ one should see $\delta > 0.73$ in case of DP universality [40], that can be excluded by the present simulations.

Below the transition point for fixed $\nu = 0.95$ we can find $P(t)$ decay curves with PL tails, characterized by the exponents $0 < \delta < 0.5$ as we vary λ between 0.845 and 0.88. In this region the avalanche size distributions also show

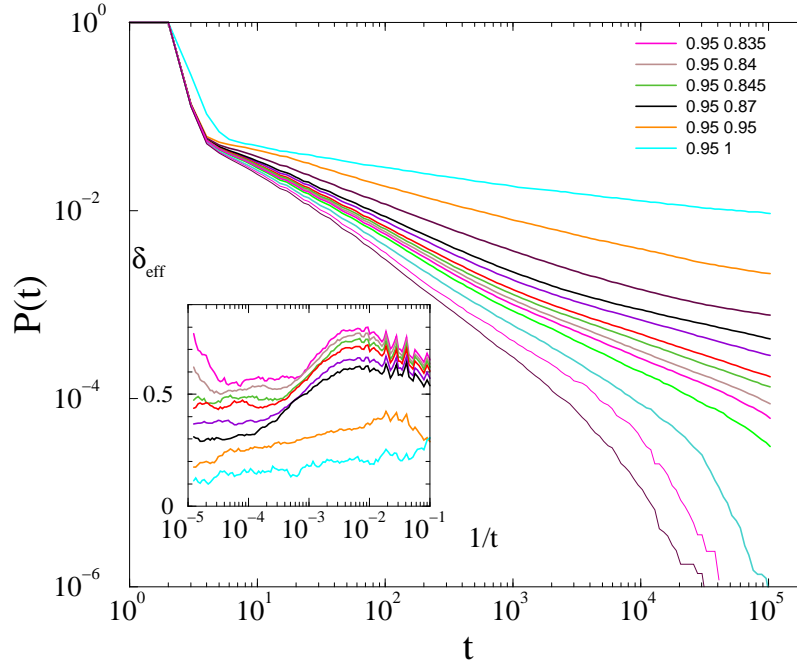


FIG. 2: Avalanche survival distribution of the relative threshold model with $K = 0.25$, for $\nu = 0.95$ and $\lambda = 0.8, 0.81, 0.82, 0.83, 0.835, 0.84, 0.845, 0.85, 0.86, 0.87, 0.9, 0.95, 1$ (bottom to top curves). Inset: Local slopes of the same from $\lambda = 0.835$ to $\lambda = 1$ (top to bottom curves).

PL decay (Fig. 3), modulated by some oscillations due to the modular network structure, but the slope of curves is around $\tau = 1.26(2)$, a smaller value than obtained by the brain experiments: $\tau \simeq 1.5$ [1].

I have also tested the collapse of averaged avalanche distributions $\Pi(t)$ of fixed temporal sizes T as in [42]. The inset of Fig. 3 shows good a collapse, obtained for avalanches of temporal sizes $T = 25, 63, 218, 404$ and using a vertical scaling $\Pi(t)/T^{0.34}$, which is near to the experimental findings reported in [42]. Note, the asymmetric shapes, which are also in agreement with the experiments and could not be reproduced by the model of ref. [42].

To test the robustness of the results I also run simulations on the KKI-18 network with fully unidirectional edges at $K = 0.25$. I obtained very similar PL tails as before, but for the same control parameters the slopes of $\ln[P(\ln t)]$ curves were bigger, meaning that in the diluted networks the avalanches survive for longer times. The avalanche size

distributions also fell down faster, i.e. $1.6 < \tau < 2$.

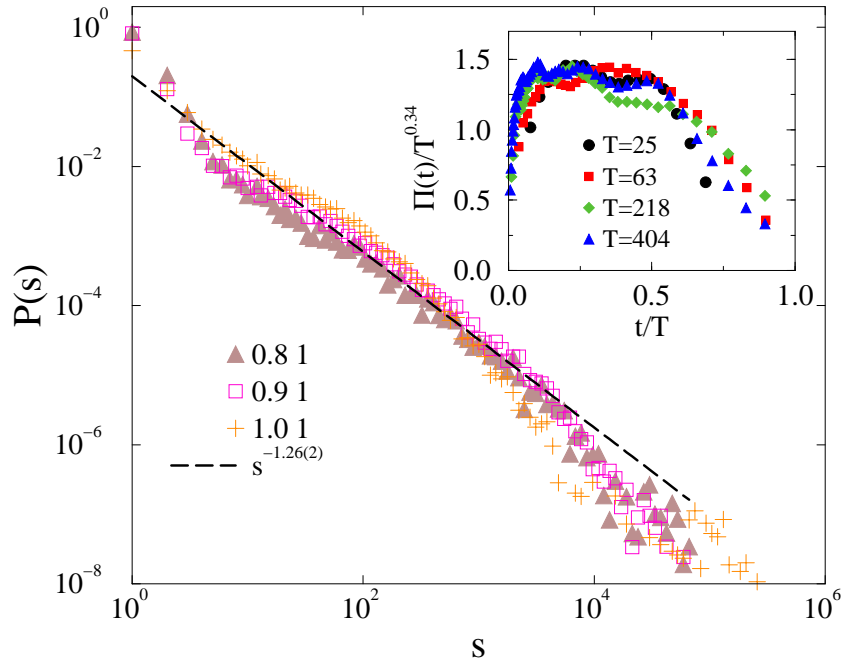


FIG. 3: Avalanche size distribution of the relative threshold model with $K = 0.25$, for $\nu = 1$ and $\lambda = 1, 0.9, 0.8$. Dashed line: PL fit to the $\lambda = 0.8$ case. Inset: Avalanche shape collapse for $T = 25, 63, 218, 404$ at $\lambda = 0.86$ and $\nu = 0.95$

In real brain networks inhibitory connections also happen. To model this I changed the signs of certain portion of the weights randomly. This produces further heterogeneity, thus stronger rare-region effects. Figure 4 shows the survival probabilities, when 30% of the links turned to inhibitory for $K = 0.1$ and $\lambda = 0.95$. The critical point, above which $P(t)$ signals persistent activity, is around $\nu = 0.57$, very hard to locate clearly, since the evolution slows down and exhibit strong (oscillating) corrections. Below the transition point the survival exponent changes continuously as $0 < \delta < 0.5$ for the response for the variation of ν between $\simeq 0.5$ and $\simeq 0.57$ (inset of Fig. 4). Now the avalanche size distributions (Fig. 5) exhibit PL tails with $\tau \simeq 1.5$, close to the experimental value for brain [1]. A slight change of τ can also be observed by varying the control parameter below the critical point. This variation can be seen even better on the exponent η , which is related to τ via Eq. 7 (inset of Fig. 5), thus Griffiths effects could easily be tested by measuring this. Using 20% of inhibitory links I obtained the same τ -s, while in case of 10% inhibition I obtained $\tau \simeq 1.3$ at the critical point.

For a higher threshold values (like $K = 0.2, 0.25$) the critical point shifts to smaller ν parameters and the Griffiths effects are still visible. However, the avalanche size distributions exhibit a faster decay, characterized by: $\tau \simeq 1.7 - 2$.

IV. CONCLUSIONS

I studied the possibility of slow, PL dynamics in case of threshold models without the assumption of a SOC mechanism. I used a large human brain connectome graph downloaded from the OCP site. The network heterogeneity was found to be strong enough to round the phase transition on a 3d homogeneous lattice and cause non-universal PL-s in the case of models, where the sensitivity of nodes are kept constant. These Griffiths effects occur in extended control parameter spaces.

On the other hand for constant threshold models rare region effects are too weak to change the 3d lattice dynamical behavior in contrast with other recent publications on connectomes [20]. This study presents systematic simulations of much larger sizes than before. While the inclusion of a 20% edge directness does not affect the results qualitatively, changing signs of weights brings them closer to reality. In particular the introduction of 20 – 30% of inhibitory links, selected randomly, results in distributions of avalanche sizes and times that agree with the neural experiments. Besides the scaling in an extended control parameter space below the critical point the scaling exponents vary with them slightly as the consequence of rare region effects. Strong and oscillating corrections to scaling were pointed out,

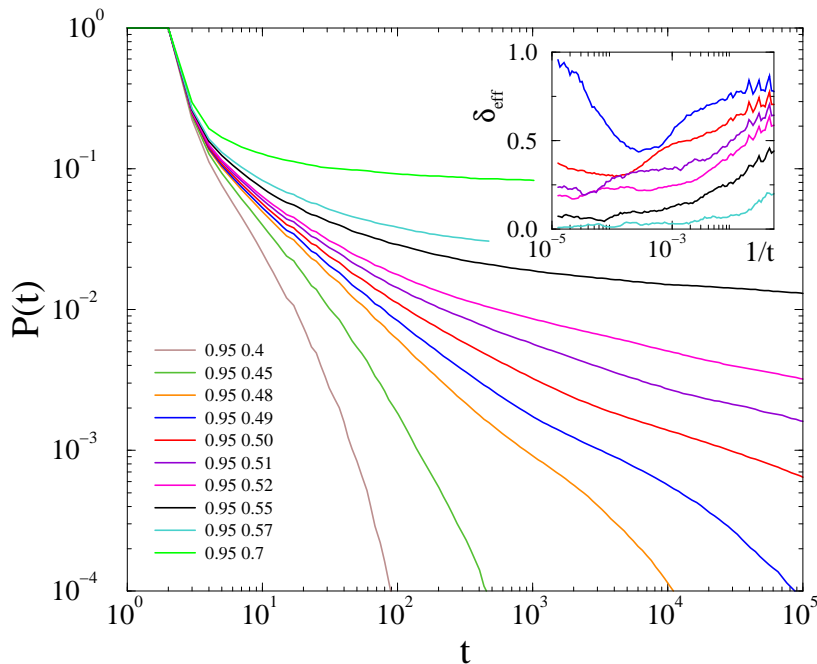


FIG. 4: Avalanche survival distribution of the relative threshold model with 30% inhibitory links at $K = 0.1$, for $\lambda = 0.95$ and $\nu = 0.4, 0.45, 0.49, 0.5, 0.51, 0.52, 0.55, 0.57, 0.7$ (bottom to top curves). Inset: Local slopes of the same curves in opposite order.

which emerge as the result of the modular structure of the connectome. As an earlier study showed some universality of the OCP graph topologies [24] one can expect the same dynamical behavior on them using this model.

The GP effects shown here are obtained at high reaction probabilities that are assumed for optimal brain function. It is important to note that while some rough tuning of the control parameters might be necessary to get closer to the critical point one can see dynamical criticality even **in the inactive phase**, which is a very reliable and safe expectation for a brain system [43]. Recent experiments suggest slightly sub-critical brain states in vivo, devoid of dangerous over-activity linked to epilepsy.

One can debate the assumption of relative threshold model, that was found to be necessary to see PL-s. However, inhibitory weights increase the heterogeneity drastically, such that a full equalization of the internal sensitivity may not be obligatory to find Griffiths effects. The negative weights enable local sustained activity and promote strong rare region effects without a network fragmentation.

As a next step one could study the application of more elaborated brain models, like the introduction of refractory times or considering Kuramoto oscillators operating on patches of neurons (nodes of these graphs), but we can expect very similar Griffiths effects as shown here. The assumption of quasi-static can also be relaxed by allowing time dependent link/weight structures.

Acknowledgments

I thank the useful discussions to C.C. Hilgetag and R. Juhász and comments to M. A. Muñoz. Support from the Hungarian research fund OTKA (Grant No. K109577) is acknowledged.

-
- [1] J. Beggs and D. Plenz, *Neuronal avalanches in neocortical circuits*, J. Neurosci., **23**, (2003) 11167.
 - [2] C. Tetzlaff et al., *Self-Organized Criticality in Developing Neuronal Networks*, PLoS Comput. Biol. **6**, (2010) e1001013.
 - [3] G. Hahn et al., *Neuronal avalanches in spontaneous activity in vivo*, J. Neurophysiol. **104**, (2010) 3312.
 - [4] T. L. Ribeiro et al., *Spike Avalanches Exhibit Universal Dynamics across the Sleep-Wake Cycle*, PLoS ONE **5**, (2010), e14129
 - [5] for a review see R. Legenstein and W. Maass, *New Directions in Statistical Signal Processing: From Systems to Brain*, eds S. Haykin, J. C. Principe, T. Sejnowski, J. McWhirter (Cambridge, MIT Press), 127154.

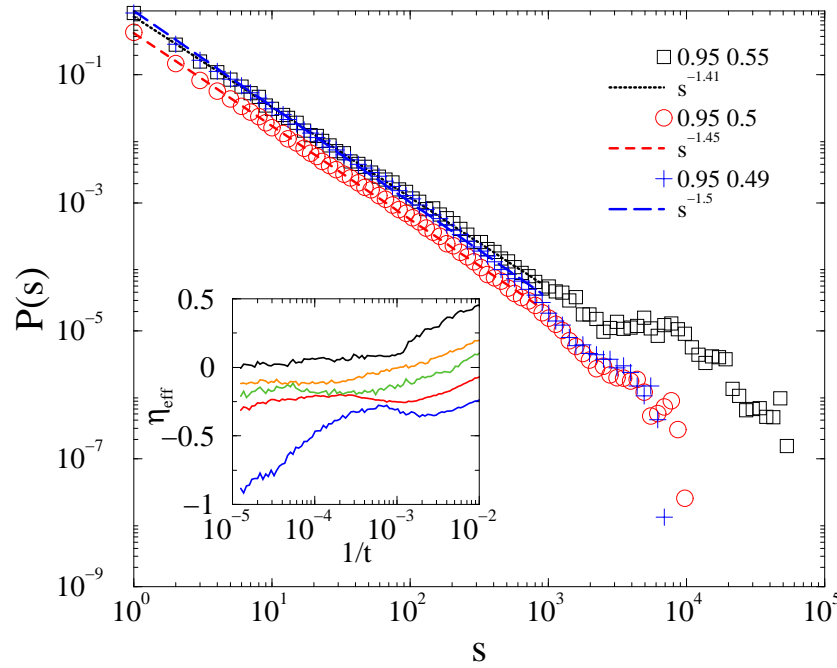


FIG. 5: Avalanche size distribution of the relative threshold model with 30% inhibitory links at $K = 0.1$, $\nu = 0.95$ and $\lambda = 0.49, 0.5, 0.55$. Dashed lines: PL fits. Inset: Effective η exponent for $\nu = 0.95$ and $\lambda = 0.49, 0.5, 0.51, 0.51, 0.55$ (bottom to top curves).

- [6] P. Bak, C. Tang and K. Wiesenfeld, *Self-organized criticality*, Phys. Rev. A **38**, (1988) 364374.
- [7] G. Pruessner, *Self Organized Criticality*, Cambridge University Press, Cambridge 2012.
- [8] J. Hidalgo et al., PNAS **111**, 10095-10100 (2014).
- [9] T. Vojta, *Rare region effects at classical, quantum and nonequilibrium phase transitions*, J. Physics A: Math. and Gen. **39**, R143 (2006).
- [10] P. M. Villa Martin, J. A. Bonachela and M.A. Muñoz, *Quenched disorder forbids discontinuous transitions in nonequilibrium low-dimensional systems*, Phys. Rev. E **89**, (2014) 012145.
- [11] P. M. Villa Martin, M. Moretti and M.A. Muñoz, *Rounding of abrupt phase transitions in brain networks*, J. Stat. Mech. (2015) P01003.
- [12] R. B. Griffiths, *Nonanalytic Behavior Above the Critical Point in a Random Ising Ferromagnet*, Phys. Rev. Lett. **23**, 17 (1969).
- [13] G. Ódor, *Slow, bursty dynamics as a consequence of quenched network topologies*, Phys. Rev. E **89**, 042102 (2014)
- [14] S. Johnson, J. J. Torres, and J. Marro, *Robust Short-Term Memory without Synaptic Learning*, PLoS ONE **8**(1): e50276 (2013)
- [15] M. A. Muñoz, R. Juhász, C. Castellano and G. Ódor, *Griffiths phases on complex networks*, Phys. Rev. Lett. **105** (2010) 128701.
- [16] Harris T. E., *Contact Interactions on a Lattice*, Ann. Prob. **2**, 969-988 (1974).
- [17] G. Ódor and R. Pastor-Satorras, *Slow dynamics and rare-region effects in the contact process on weighted tree networks*, Phys. Rev. E **86**, (2012) 026117.
- [18] G. Ódor, *Rare regions of the susceptible-infected-susceptible model on Barabasi-Albert networks*, Phys. Rev. E **87**, (2013) 042132.
- [19] G. Ódor, *Spectral analysis and slow spreading dynamics on complex networks*, Phys. Rev. E **88**, (2013) 032109.
- [20] P. Moretti, M. A. Muñoz, *Griffiths phases and the stretching of criticality in brain networks*, Nature Communications **4**, (2013) 2521.
- [21] P. Villegas, P. Moretti and Miguel A. Muñoz, Scientific Reports **4**, 5990 (2014)
- [22] G. Ódor, R. Dickman and G. Ódor, *Griffiths phases and localization in hierarchical modular networks*, Sci. Rep. 2015 14451.
- [23] W. Cota, S. C. Ferreira, G. Ódor, *Griffiths effects of the susceptible-infected-susceptible epidemic model on random power-law networks*, Phys. Rev. E **93**, 032322 (2016).
- [24] M. T. Gastner and G. G. Ódor, *The topology of large Open Connectome networks for the human brain*, arXiv:1512.01197.
- [25] See: <http://www.openconnectomeproject.org>
- [26] Bennett A. Landman et al, NeuroImage **54** (2011) 28542866.
- [27] P. Hagmann, et al. *Mapping the Structural Core of Human Cerebral Cortex*. PLoS Biol. **6**, e159 (2008).

- [28] C. J. Honey, et al. *Predicting human resting-state functional connectivity from structural connectivity*, Proc. Natl. Acad. Sci. **106**, 20352040 (2009).
- [29] W. G. Roncal et al., *MIGRAINE: MRI Graph Reliability Analysis and Inference for Connectomics*, preprint: arXiv.org:1312.4875.
- [30] D. J. Felleman and D. C. Van Essen, *Distributed hierarchical processing in the primate cerebral cortex*, Cerebr. Cortex, **1**, (1991), 147.
- [31] N. T. Markov et al., Cerebr. Cortex, **24**, (2012), 17-36.
- [32] M. Kaiser and C. C. Hilgetag, *Optimal hierarchical modular topologies for producing limited sustained activation of neural networks*, Front. in Neuroinf., **4** (2010) 8.
- [33] R. Azouz and C. M. Gray, PNAS **97**, 8110 (2000).
- [34] M.-T. Hütt, M. K. Jain , C. C. Hilgetag, A. Lesne, Chaos, Solitons & Fractals, **45**, 611 (2012).
- [35] P. Grassberger and A. de la Torre, Ann. Phys. **122**, 373 (1979).
- [36] M. A. Munoz, R. Dickman, A. Vespignani and S. Zapperi, Phys. Rev. E **59**, 6175 (1999).
- [37] G. Ódor, Phys. Rev. E **67**, 056114 (2003).
- [38] I. A. Kovács, F. Iglói, Phys. Rev. B **83**, 174207 (2011).
- [39] T. Vojta, Phys. Rev. E **86**, 051137 (2012).
- [40] G. Ódor, Rev. Mod. Phys. **76**, 663 (2004).
- [41] J. Marro and R. Dickman, *Nonequilibrium phase transitions in lattice models*, Cambridge University Press, Cambridge, 1999.
- [42] N. Friedman et al., Phys. Rev. Lett. **108**, 208102 (2012).
- [43] V. Priesemann et al, Front. in Sys. NeuroSci. **8** (2014) 108.